# The Distribution of Sugar Chains on the Vomeronasal Epithelium Observed with an Atomic Force Microscope

**Toshiya Osada, Shinichiro Takezawa, Arimichi Itoh, Hideo Arakawa, Masumi Ichikawa[1] and Atsushi Ikai**

Department of Biological Sciences, Faculty of Bioscience and Biotechnology, Tokyo Institute of Technology, Nagatsuta, Midori-ku, Yokohama 226-0026 and [1]Anatomy and Embryology, Tokyo Metropolitan Institute for Neuroscience, Fuchu, Tokyo 183-8526, Japan

*Correspondence to be sent to: Dr Toshiya Osada, Department of Biological Sciences, Faculty of Bioscience and Biotechnology, Tokyo Institute of Technology, 4259 Nagatsuta, Midori-ku, Yokohama 226-0026, Japan. e-mail: tosada@bio.titech.ac.jp*

## Abstract

The distribution of sugar chains on tissue sections of the rat vomeronasal epithelium, and the adhesive force between the sugar and its specific lectin were examined with an atomic force microscope (AFM). AFM tips were modified with a lectin, *Vicia villosa* agglutinin, which recognizes terminal *N*-acetyl-D-galactosamine (GalNAc). When a modified tip scanned the luminal surface of the sensory epithelium, adhesive interactions between the tip and the sample surface were observed. The final rupture force was calculated to be ~50 pN based on the spring constant of the AFM cantilever. Distribution patterns of sugar chains obtained from the force mapping image were very similar to those observed using fluorescence-labeled lectin staining. AFM also revealed distribution patterns of sugar chains at a higher resolution than those obtained with fluorescence microscopy. Most of the adhesive interactions disappeared when the scanning solution contained 1 mM GalNAc. The adhesive interactions were restored by removing the sugar from the solution. Findings suggest that the adhesion force observed are related to the binding force between the lectin and the sugars distributed across the vomeronasal epithelium.

## Introduction

The atomic force microscope (AFM) was developed as a scanning probe microscope which gives high resolution images by recording interactions between the scanning probe and sample surface (Binnig *et al.*, 1982, 1986). Recently, AFM images using biological materials have been reported. For example, the typical circular structure of plasmid DNAs and complexes between DNA and proteins have been resolved with the AFM (Bustamante, *et al.*, 1992; Vesenka *et al.*, 1992; Hansma and Hoh, 1994). Other biological materials such as proteins (Weisenhorn *et al.*, 1990; Hallett *et al.*, 1995), viruses (Ikai *et al.*, 1993; Imai *et al.*, 1993) and cell surfaces (Paul *et al.*, 1994; Eppell *et al.*, 1995) have been extensively studied with the AFM. The AFM can be used for both conductive and insulating materials both in liquid and in air (Lal and John, 1994), which allows the AFM to be used in biological systems such as RNA polymerase activity (Kasas *et al.*, 1997), the clotting process of fibrinogen (Drake *et al.*, 1989) and cell growth of yeast cells (Gad and Ikai, 1995). As the AFM tip comes into contact with the sample surface, physical properties of the sample as well as its topography can be obtained (Ikai, 1996; Mitsui *et al.*, 1996; Brown and Hoh, 1997; Oberleithner *et al.*, 1997; Rief *et al.*, 1997). AFM can also be used to measure specific forces between the probe tip and the sample surface. It is possible to measure the forces between the sample surface and any material selected by modifying the AFM tip with that material. It has been shown that the binding forces between DNA base pairs (Boland and Ratner, 1995), avidin and biotin (Lee *et al.*, 1994; Ludwig *et al.*, 1997), ligand and receptor (Florin *et al.*, 1994; Moy *et al.*, 1994) and antigen and antibody (Dammer *et al.*, 1996; Hinterdorfer *et al.*, 1996; Allen *et al.*, 1997; You *et al.*, 1997) can be measured using an AFM.

The vomeronasal organ is located at the base of the nasal septum and originates from the olfactory placode. The neuroepithelium of the vomeronasal organ (Wysocki, 1979; Halpern, 1987) is similar in structure to the olfactory epithelium, consisting of supporting cells, receptor neurons and precursor cells. The vomeronasal organ functions to detect substances such as pheromones associated with social and reproductive behaviors. These substances may be detected by receptors which are most likely located on the microvillar surface of vomeronasal sensory neurons.

In a previous paper (Osada *et al.*, 1998) we described a new method for the preparation of vomeronasal tissue sections which allowed us to obtain AFM images com-

parable to images obtained using the transmission electron microscope (TEM). Most subcellular structures of the vomeronasal epithelium observed with the TEM were also observed with the AFM. In this report we describe another potential AFM application for the study of the vomeronasal organ. As the AFM tip makes contact with the sample surface, it is possible to measure the binding force between pheromone substances and their receptors. Since rat pheromones are not yet available, we used *Vicia villosa* agglutinin (VVA), which is reported to label the luminal surface of vomeronasal sensory epithelium (Takami *et al.*, 1994).

## Materials and methods

### Tissue sections

Sprague–Dawley rats were anesthetized with sodium pentobarbital (50 mg/kg, i.p.) and perfused with physiological saline followed by fixation with 4% paraformaldehyde in 0.1 M phosphate buffer. The vomeronasal organs were removed and kept in the fixative solution overnight. The organs were cut into 20-μm-thick sections using a freezing microtome. Sections were mounted onto gelatin-coated slides and stored at –80°C until used.

### Lectin staining

The sample sections were rinsed with phosphate-buffered saline (PBS) and then incubated with fluorescein isothiocyanate (FITC)-labeled VVA (Sigma, St Louis, MO) for 1 h followed by washing in three changes of PBS for at least 10 min each. Sections were coverslipped with water-based mountant (PermaFlour Lipshaw) and observed with a confocal laser scanning microscope (MRC-600, Bio-Rad, Tokyo, Japan).

### Preparation of AFM tips

Free sulfhydryl groups were introduced onto VVA by derivatization with long-chain succinimidyl 6-[3′-(2-pyridyldithio)-propionamido] (Pierce, IL, USA) followed by the reduction with dithiothreitol (DTT). The sample solution was applied to Sephadex G-25 (Pharmacia, Uppsala, Sweden) to remove DTT. About four thiol groups were introduced on VVA as estimated from the determination of generated pyridine-2-thione with a spectrophotometer. Gold-coated AFM tips (OMCL-TR400PB; OLYMPUS, Tokyo, Japan) with a nominal spring constant of 0.025 N/m were modified with the derived VVA through Au–S bonds.

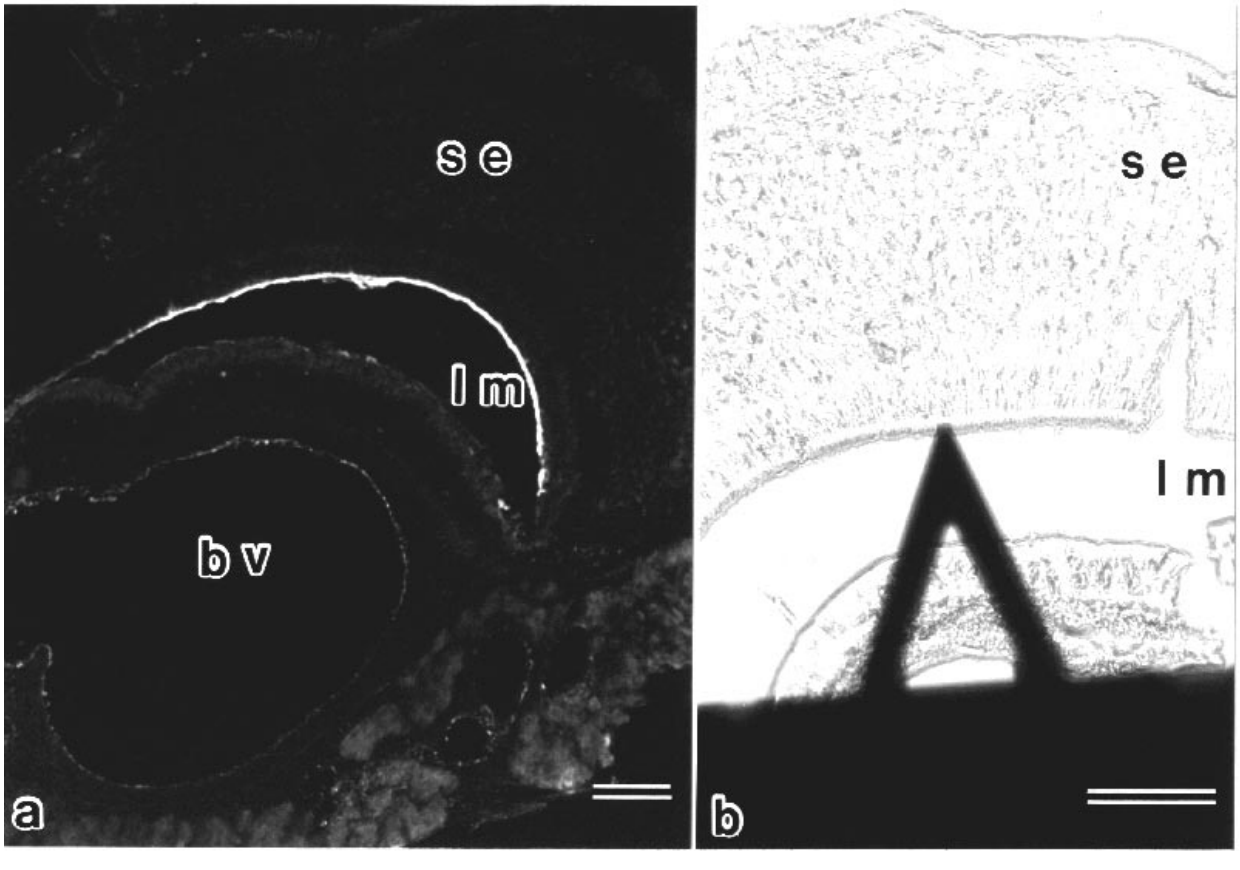


**Figure 1** **(a)** Binding of FITC-labeled VVA in a histological section of the rat vomeronasal organ. Very intense fluorescence is present in the microvilli surface of the sensory epithelium. The sensory epithelium (se), the lumen (lm) and a blood vessel (bv) can be seen. **(b)** Photomicrograph of an AFM cantilever over a histological section of the rat vomeronasal organ. A tip which is mounted on the end of the cantilever scans the sample surface. Scale bar = 100 μm.

### Atomic force microscopy

AFM was performed in force volume mode using an NVB100 AFM (OLYMPUS) in combination with an inverted optical microscope. All experiments were done in Petri dishes filled with PBS. The scan area was divided into 16 × 16 sub-areas, where force curves were obtained in each sub-area. Both the horizontal and vertical scan rates were 1 Hz. The maximum pressure between the tip and the sample surface was controlled using the trigger mode, so that the maximum bending of the cantilever was limited to 10 nm.

## Results

In previous studies FITC-labeled VVA was reported to stain only the microvillar surface of the vomeronasal sensory epithelium (Takami *et al.*, 1994). Figure 1a confirms these results and illustrates the intense fluorescence observed at the microvillar surface. Figure 1b shows an AFM cantilever over the section of the vomeronasal epithelium with a tip located at its end, although this cannot be seen in the figure. The position of the tip was controlled using an optical microscope.

Figure 2a shows a schematic drawing of the AFM force curve. The ordinate is the deflection of the cantilever and the abscissa is the distance moved by the piezoelectronics that drives the cantilever up or down relative to the sample surface. When the cantilever approaches, the force curve is initially flat until it reaches the sample surface, where it starts to be deflected linearly. After the cantilever starts to retract at the left end of the diagram, the curve closely follows the previous approach curve until the deflection returns to the initial level. When the cantilever is withdrawn, the adhesion force between the tip and the surface causes the cantilever to bend towards the sample for some distance. This distance can be used to estimate the rupture force required to break the adhesion (force = II × spring constant of the cantilever). The length of the sugar chain pulled by cantilever can be obtained by subtracting II from I. Force curves were obtained from 256 sub-areas to map the distribution of the specific sugar. Force curves are classified into three categories. The first group includes force curves with rupture events (Figure 2b), which indicates adhesion events between the lectin molecules and sugar chains. The second group includes force curves without rupture events (Figure 2c), which shows no interaction between the tip and the sample. The last group contains force curves that appear when the tip could not reach the sample surface (data not shown). This indicates that the sample has a groove deeper than the vertical scan range (1 μm) of the force curve. These force curves were observed in this experiment when the tip scanned over the lumen of the vomeronasal epithelium.

Figure 3 shows the distribution of these three kinds of force curves. As shown in Figure 3a, b, the adhesive points were distributed at the boundary of a groove and rarely

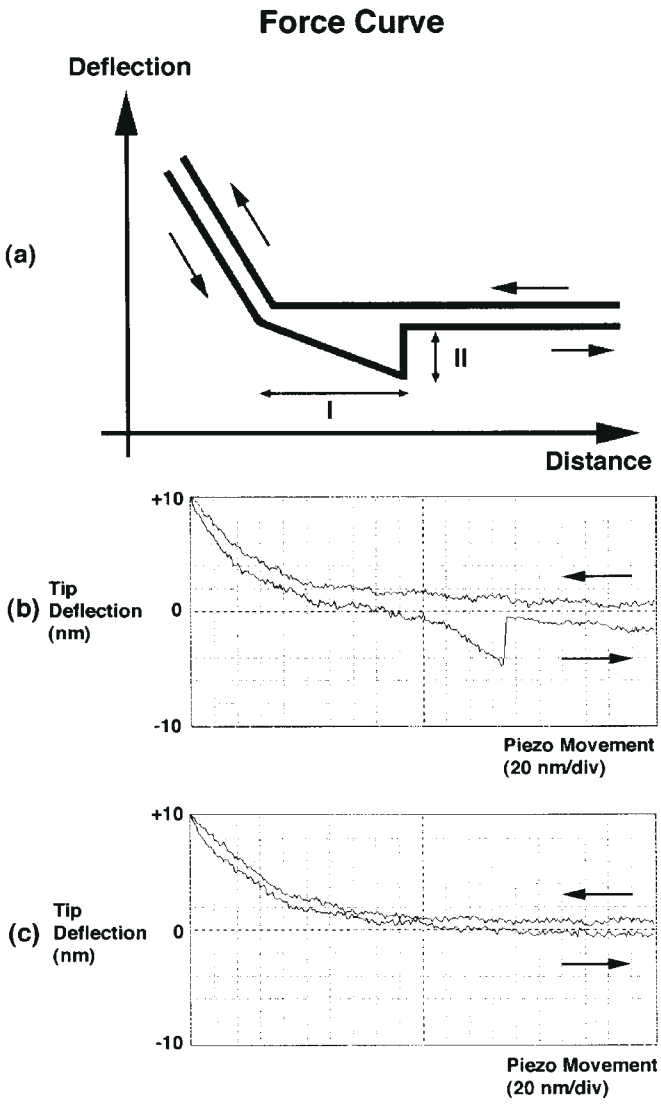


**Figure 2** **(a)** Schematic drawing of an AFM force curve. Typical examples of force curves are shown in **(b)** and **(c)**. In (b), the retrace line of the force curve shows adhesion force between the tip and the sample, which represents the VVA–GalNAc interaction. In contrast, (c) shows no interaction, which indicates GalNAc was not present.

existed on internal area as one can see in Figure 3c. The distributions shown in Figure 3a, b were reproduced in sequential scanning of the same area. Based on microscopic observation of the tip position during force mapping, it was determined that the zone of adhesion was on the microvillar surface of the sensory epithelium. The distribution of the adhesion observed with AFM corresponded to the fluorescence image in Figure 1a, except that the AFM adhesion zone seemed to make two lines where the fluorescence did not. To confirm this result we observed the VVA FITC-stained tissue section using a confocal microscope. When we focused on a thin layer at the top surface of the sample, we observed two lines of fluorescence (Figure 3d).

In order to confirm that the observed adhesion was due

to the specific binding of the lectin to *N*-acetyl-D-galactosamine (GalNAc), a competitive experiment was carried out. Figure 4a shows the force mapping within a 500 × 500 nm scanning area in the adhesive zone. Then GalNAc (1 mM) in PBS was added to the Petri dish and incubated for 30 min at room temperature. The frequency of the adhesion was dramatically decreased, as shown in Figure 4b. The adhesion was recovered after the solution in the Petri dish was washed with PBS three times. Given these observations, together with the results illustrated in Figure 3 showing the position specificity of the adhesion, we concluded that the measured adhesion force was due to specific binding between VVA and GalNAc.

The advantage of using AFM to detect ligand distribution lies not only in its high resolution but also in its ability to detect the strength of the binding and the length of the interaction. We analyzed the force curves that show rupture events from this point of view. The binding force and length were determined as shown in Figure 2a. The histogram of the binding force (Figure 5a) showed a peak around 50 pN. This value represents the force needed to rupture the binding between the lectin and the sugar. Some very strong rupture

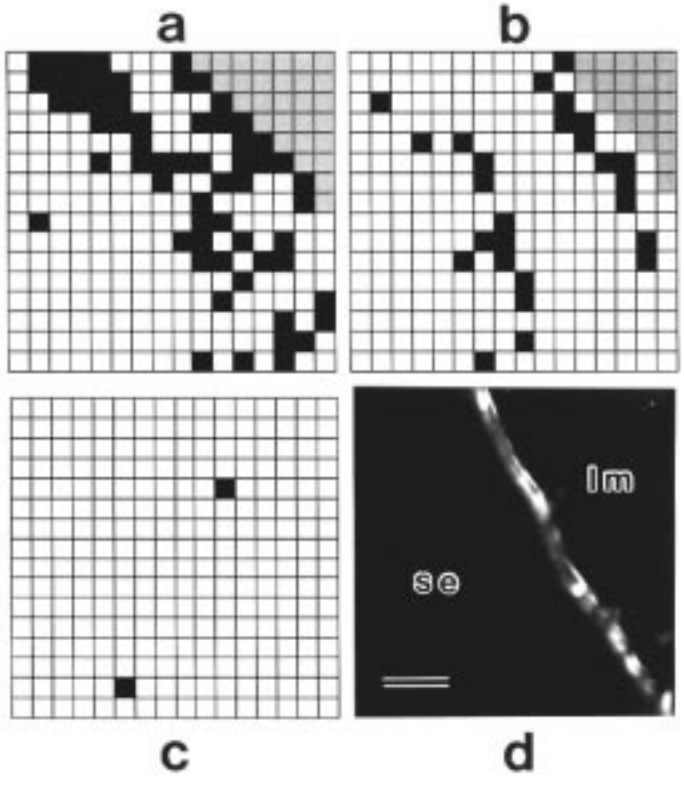


**Figure 3** Distribution of adhesion force between the tip and the surface of the histological section **(a, b, c)**. Each black pixel was interpreted as representing a position where GalNAc was present. Gray pixels indicate the lumen of the vomeronasal epithelium. (a) and (b) reveal that GalNAc is present at the microvillar surface. (c) shows the force mapping image on sensory epithelium, where there were few detected adhesions. These images show the force mapping in a 10 × 10 μm scanning area. To confirm the results of (a) and (b), we observed the VVA FITC-stained tissue section using confocal microscopy. When we focused on a thin layer of the top surface, two lines of fluorescence were observed **(d)**. Scale bar = 50 μm.

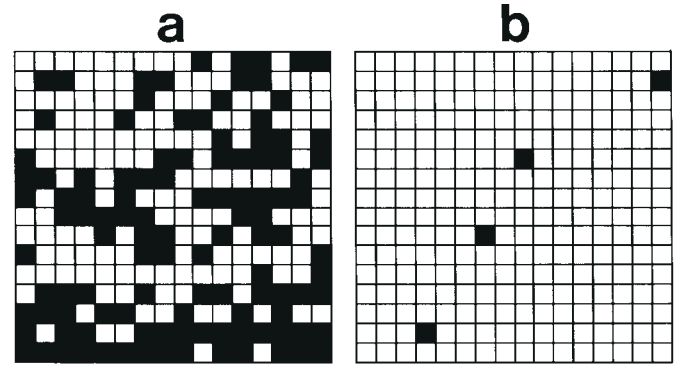


**Figure 4** In order to clarify that the observed adhesion is due to the specific binding of the VVA to GalNAc, a competitive binding experiment was carried out. **(a)** The force mapping in the adhesive zone (500 × 500 nm). Then GalNAc (1 mM) was added to the Petri dish and incubated for 30 min. The frequency of the adhesions detected was dramatically decreased, as shown in **(b)**. The adhesion recovered after the solution was replaced with PBS.

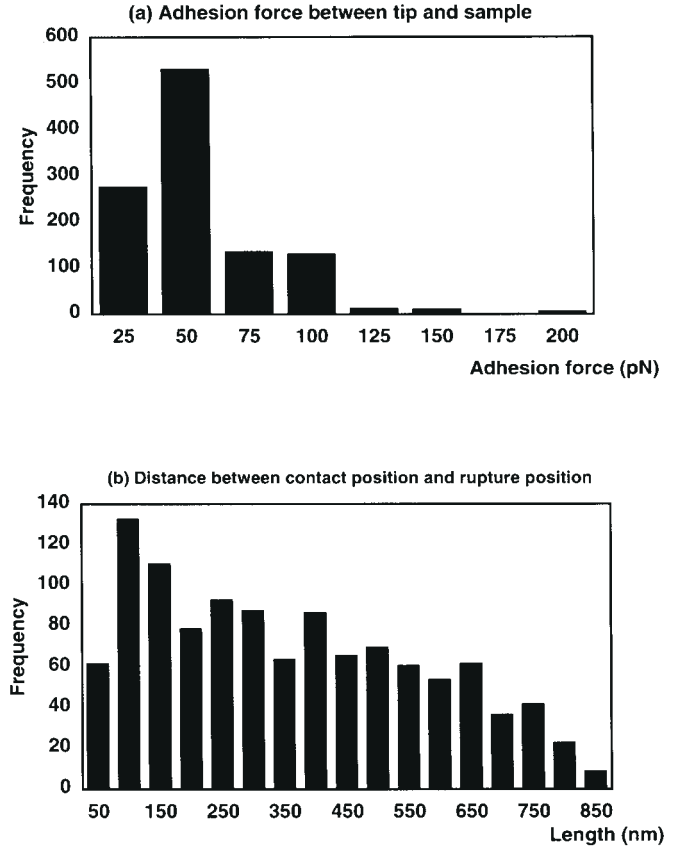


**Figure 5** Histogram of binding forces showing a peak around 50 pN **(a)**. This value represents the force needed to rupture the binding force between VVA and GalNAc. The histogram of the length showed a more dispersed distribution, which indicates that the bound sugar chains were pulled for some length **(b)**.

forces may represent a multiple binding effect. The histogram of the length (Figure 5b) showed a more dispersed distribution, suggesting that the bound sugar chains were pulled for some length (~800 nm).

## Discussion

AFM tips modified with VVA have been employed to map the distribution of terminal GalNAc on vomeronasal epithelial sections. The results shown in Figure 3a, b illustrate the high resolution of specific sugar mapping with an AFM. The distribution of the sugar forming two bands was not seen with fluorescence microscopy. This illustrates the unique potential of the AFM method in determining the fine distribution of ligands or receptors. Findings suggest that GalNAc is enriched in the apical and basal thirds of microvilli but not in middle third. This distribution pattern of sugars has not been reported before. However, we cannot exclude the possibility that these are artificial structures due to sample preparation.

When the epithelial sections were mapped with only the gold-coated AFM tips without any modification, many adhesion forces were observed randomly (data not shown). This is due to non-specific interaction between gold and the sample surface as reported previously (Allen *et al.*, 1997). When the gold-coated AFM tips were modified with bovine serum albumin or other lectins which cannot stain vomeronasal epithelial sections, the non-specific interactions disappeared (data not shown). The modified tip with VVA can be used not only to detect specific binding between VVA and the sugar but also to reduce non-specific binding between gold and the sample surface. We confirmed that the adhesive forces observed here was specific binding between VVA and the sugar using competitive experiments, as shown in Figure 4.

Figure 5 suggests that this method has the ability to examine properties of the detected binding. As we succeeded in measuring binding forces, it is possible to distinguish and compare the sites with different binding forces. This is important when several similar receptors with different binding forces to the same ligand are distributed in a tissue. Our method will open a new way to map individual receptors. The length of interaction was distributed divergently. This may come from the wide distribution of the length of the detected sugar chains. The other possibility is that the membrane where the sugar chains were anchored was deformed differently when pulled. Further investigation is needed to determine the cause of the observed distribution. This method may be useful for examining the interaction between pheromone and its receptor and the distribution of the receptors on the luminal surface of the sensory epithelium.

## Acknowledgements

The authors thank Dr R. Costanzo for critically reviewing the manuscript and for helpful discussion. We also thank N. Iwasaki for her technical assistance. This research was supported by CREST (J.S.T.).

## References

**Allen, S., Chen, X., Davies, J., Davies, M.C., Dawkes, A.C., Edwards, J.C., Roberts, C.J., Sefton, J., Tendler, S.J.B.** and **Williams, P.M.** (1997) *Detection of antigen–antibody binding events with the atomic force microscope*. Biochemistry, 36, 7457–7463.

**Binnig, G., Quate, C.F., Gerber, C.H.** and **Weibel, E.** (1982) *Surface studies by scanning tunneling microscopy*. Phys. Rev. Lett., 49, 57–61.

**Binnig, G., Rohrer, H.** and **Gerber, C.H.** (1986) *Atomic force microscopy*. Phys. Rev. Lett., 56, 930–933.

**Boland, T.** and **Ratner, B.D.** (1995) *Direct measurement of hydrogen binding in DNA nucleotide bases by atomic force microscopy*. Proc. Natl Acad. Sci. USA, 92, 5297–5301.

**Brown, H.G.** and **Hoh, J.H.** (1997) *Entropic exclusion by neurofilament sidearms: a mechanism for maintaining interfilament spacing*. Biochemistry, 36, 15035–15040.

**Bustamante, C.J., Vesenka, J., Tang, C.L., Rees, W., Guthold, M.** and **Keller, R.** (1992) *Circular DNA molecules imaged in air by scanning force microscopy*. Biochemistry, 31, 22–26.

**Dammer, U., Hegner, M., Anselmetti, D., Wagner, P., Dreier, M., Huber, W.** and **Guntherodt, H.J.** (1996) *Specific antigen/antibody interaction measured by force microscopy*. Biophys. J., 70, 2437–2441.

**Drake, B., Orater, C.B., Weisenhorn, A.L., Gould, S.A.C., Albrecht, T.R., Quate, C.F., Cannell, D.S., Hansma, H.G.** and **Hansma, P.K.** (1989) *Imaging crystals, polymers and processes in water with the atomic force microscope*. Science, 243, 1586–1589.

**Eppell, S.J., Simmons, S.R., Albrecht, R.M.** and **Marchant, R.E.** (1995) *Cell surface receptors and proteins of platelet membranes imaged by scanning force microscopy using immunogold contrast enhancement*. Biophys. J., 68, 671–680.

**Florin, E.L., Moy, V.T.** and **Gaub, H.E.** (1994) *Adhesion forces between individual ligand pairs*. Science, 264, 415–417.

**Gad, M.** and **Ikai, A.** (1995) *Method for immobilizing microbial cells on gel surface for dynamic AFM studies*. Biophys. J., 69, 2226–2233.

**Hallett, P., Offer, G.** and **Miles, M.T.** (1995) *Atomic force microscopy of the myosin molecule*. Biophys. J., 68, 1604–1606.

**Halpern, M.** (1987) *The organization and function of the vomeronasal system*. Annu. Rev. Neurosci., 10, 325–362.

**Hansma, H.G.** and **Hoh, J.** (1994) *Biomolecular imaging with the atomic force microscope*. Annu. Rev. Biophys. Biomol. Struct., 23, 115–139.

**Hinterdorfer, P., Baumgartner, W., Gruber, H.J., Schilcher, K.** and **Schindler, H.** (1996) *Detection and localization of individual antibody–antigen recognition events by atomic force microscopy*. Proc. Natl Acad. Sci. USA, 93, 3477–3481.

**Ikai, A., Yoshimura, K., Arisaka, F., Ritani, A.** and **Imai, K.** (1993) *Atomic force microscopy of bacteriophage T4 and its tube–baseplate complex*. FEBS Lett., 326, 39–41.

**Ikai, A.** (1996) *STM and AFM of bio/organic molecules and structure*. Surface Sci. Rep., 26, 261–332.

**Imai, K., Yoshimura, K., Tomitori, M., Nishikawa, O., Kokawa, R., Yamamoto, M., Kobayashi, M.** and **Ikai. A.** (1993) *Scanning tunneling and atomic force microscopy of T4 bacteriophage and tobacco mosaic viruses*. Jpn. J. Appl. Phys., 32, 2962–2964.

**Kasas, S., Thomson, N.H., Smith, B.L., Hansma, H.G., Zhu, X.,**

**Guthold, M., Bustamante, C., Kool, E.T., Kashlev, M.** and **Hansma, P.K.** (1997) Escherichia coli *RNA polymerase activity observed using atomic force microscopy*. Biochemistry, 36, 461–468.

**Lal, R.** and **John, S.A.** (1994) *Biological applications of atomic force microscopy*. Am. J. Physiol., 266, C1–C21.

**Lee, G.U., Kidwell, D.A.** and **Colton R.C.** (1994) *Sensing discrete streptavidin–biotin interactions with atomic force microscopy*. Langmuir, 10, 354–357.

**Ludwig, M., Dettmann, W.** and **Gaub, H.E.** (1997) *Atomic force microscope imaging contrast based on molecular recognition*. Biophys. J., 72, 445–448.

**Mitsui, K., Hara, M.** and **Ikai, A.** (1996) *Mechanical unfolding of alpha-2-macroglobulin molecules with atomic force microscope*. FEBS Lett., 385, 29–33.

**Moy, V.T., Florin, E.L.** and **Gaub, H.E.** (1994) *Intermolecular forces and energies between ligands and receptors*. Science, 266, 257–259.

**Oberleithner, H., Schneider, S.W.** and **Henderson, R.M.** (1997) *Structual activity of a cloned potassium channel (ROMK1) monitored with the atomic force microscope: the 'molecular-sandwich' technique*. Proc. Natl Acad. Sci. USA, 94, 14144–14149.

**Osada, T., Arakawa, H., Ichikawa, M.** and **Ikai, A.** (1998) *Atomic force microscopy of histological sections using a new electron beam etching method*. J. Microsc., 189, 43–49.

**Paul, J.K., Nettikadan, S.R., Ganjeizadeh, Yamaguchi, M.** and **Takeyasu, K.** (1994) *Molecular imaging of $Na^+$, $K^+$-ATPase in purified kidney membranes*. FEBS Lett., 346, 289–294.

**Rief, M., Gautel, M., Oesterhelt, F., Fernandez, J.M.** and **Gaub, H.E.** (1997) *Reversible unfolding of individual titin immunoglobulin domains by AFM*. Science, 276, 1109–1112.

**Takami, S., Getchell, M.L.** and **Getchell, T.V.** (1993) *Lectin histochemical localization of galactose,* N-*acetylgalactosamine and* N-*acetylglucosamine in glycoconjugates of the rat vomeronasal organ, with comparison to the olfactory and septal mucosa*e. Cell Tissue Res., 277, 211–230.

**Vesenka, J., Guthold, M., Tang, C.L., Keller, D., Delaine, E.** and **Bustamante, C.** (1992) *A substrate preparation for reliable imaging of DNA molecules with the scanning force microscope*. Ultramicroscopy, 42/44, 1243–1249.

**Weisenhorn, A.L., Drake, B., Prater, C.B., Gould, S.A.C., Hansma, P.K., Ohnesorge, F., Egger, M., Heyn, S.P.** and **Gaub, H.E.** (1990) *Immobilized proteins in buffer imaged at molecular resolution by atomic force microscopy*. Biophys. J., 58, 1251–1258.

**Wysocki, C.J.** (1979) *Neurobehavioral evidence for the involvement of the vomeronasal system in mammalian reproduction*. Neurosci. Biobehav. Rev., 3, 301–341.

**You, H.** and **Yu, L.** (1997) *Investigation of the image contrast of tapping-mode atomic force microscopy using protein-modified cantilever tips*. Biophys. J., 73, 3299–3308.

*Accepted September 7, 1998*